

Computational Analysis On Flow Over A Bluff Bodied Re-Entry Vehicle

C.Satya Sandeep^[1], M. SureshKumar^[2], Sunil Jankar^[3]

Assistant professor, Department of Aerospace Engineering, Sandip University, Nashik.^[1]

H.O.D, Department of Aerospace Engineering, Sandip University, Nashik.^[2]

Assistant professor, Department of Mechanical Engineering, SCOE, Kharghar.^[3]

corresponding author: C.Satya Sandeep

Date of Submission: 15-07-2020

Date of Acceptance: 31-07-2020

ABSTRACT: Re-entry vehicles are subjected to very extreme flow conditions. Performing an experimental analysis is not only cost efficient but requires a lot of complicated equipment. In the current research a three dimensional CFD analysis had been performed over a reentry vehicle by using quadelateral mesh domain. Efficient turbulence models have been used to predict the flow by solving the fluid governing equations. Flow patterns were generated around the reentry vehicle and minimum and maximum fluid properties were predicted.

KEYWORDS: CFD analysis, Bluff body re-entry vehicle, Flow simulation.

I. INTRODUCTION

Experimentally analyzing the flow for high Mach number cases like re-entry vehicle takes lots of money and high end shock tunnels. CFD analysis gives a flow visualization which is almost very difficult to capture experimentally. Selecting an appropriate turbulence model is very much required to get accurate results. Yusuke Takahashi et al worked on investigating the mechanisms behind the discrepancies between wind tunnel observations and a flight test results of transonic flow fields around a re-entry vehicle by using a transonic wind tunnel and the computational fluid dynamics approach. They concluded that a sting behind the test models decreases the steep drag at transonic speeds and that shock waves reflected on the test-section walls of the wind tunnel generating local minimum values at supersonic speeds.^[1] Keiichiro Fujimoto and his team calculated RMS of the surface pressure deflections normalized by free-stream dynamic pressure. There experimental results were in good agreement in all locations including windward, side, and leeward region of the capsule wall. There results concluded that difference of the RMS of surface pressure fluctuations for flat-faced cylinder base is a higher

value as compared to re-entry capsule. They found a significant difference especially under the subsonic flow conditions.^[2]

Toshiyuki Suzuki and his team had developed a unique CFD code to calculate the flow pattern of a re-entry vehicle. There code successfully gave converged solutions for the integral flow equations.^[4] Yuan Xian and team had developed an implicit sub iteration NND scheme including second order in time and space to numerically simulate the unsteady flows over several hyper ballistic and re-entry vehicles in forced pitching movement. Then the time hystorogram of aerodynamic force and moment coefficients were obtained, and based on these data, the static/dynamic derivatives of pitching are fitted by integral and linear least square methods. They compared there results with the experimental data and made successful validation of their numerical method.^[5] J.M.A Longo et al in their work have stressed on the importance of the geometry of the re-entry vehicles to simulate the CFD flows. They concluded that geometrical simplifications of configurations applied in the CFD analysis incept errors in aerodynamic and aero-thermodynamic quantities comparable or even greater than those occurring due to numerical accuracy or drawback of physical modeling of the respective code. The importance of the initial grid design to obtain accurate solutions for hypersonic flow analysis was also a notable conclusion made by them.^[3] Yan Chao and team had worked on the influence of the grid dependency on the results of heat transfer computations. A wide variety of schemes, such as FDS, FVS AUSM⁺ and central finite difference, were evaluated in numerical experiments. They also compared their numerical data with experimental results to get an efficient scheme.^[4] A. Martin and I. Boyd had investigated the effect of gases produced during the depletion of the ablative materials used as main components in the re-entry vehicles. They implemented a CFD

code which includes carbon-phenolic in the air chemistry model. They implemented this code to simulate the flow of star dust re-entry vehicle and described the importance of adding more gases species to the model for accurate CFD simulation results.^[6]

A. Viviani and G. Pezzella studied the aerodynamic and aero-thermo dynamic features of re-entry vehicle carrying the crew of the space shuttle. They performed many simulations regarding the Euler's and Navier stokes equations to determine the hypersonic flow phenomena. They also compared there CFD findings with the experimental wind tunnel data to validate their work.^[7]Y. Takahashi performed analysis on electro magmatic waves plasma generated around the re-entry vehicle.He performed validation of simulation results with experimental findings. The comparison results came to a conclusion that the simulation results predict plasma attenceation of electromagnetic waves and radio frequency blackout very accurately.^[8]

Tian Wann et all have simulated the flow subjected to magnetic hydro dynamic power generation during the re-entry. They also simulated the thermal ionization of potassium to increase the conductivity. They made a model combining the ionization and conservation equations which predicted the results accurately.^[9]

II. DESIGN AND GRID GENERATION

Figure 1 describes all the perspective views of the re-entry vehicle. The design of the vehicle was based on the design of the Apollo re-entry shuttle. The main concentration of the work was to find out the pressure, temperature excreted on the vehicle during the atmospheric free fall. The student version of CATIA software was used to design the re-entry bluff body vehicle.The vehicle was enclosed inside a computational domain with -0.162 m and 0.162 m in X-and Y-axis. -0.052 m and 0.123 m were the limits of the computational domain in the Z axis. Generation of the mesh file is one of the important criteria which helps out a lot in generation of the efficient results. The basic mesh dimension was taken as 62*62*52 in the 3 axes, with total number of 199888 cells out of which 198580 were fluid cells, 588 solid cells and 720 partial cells. Figure 2 shows the grid file generated.

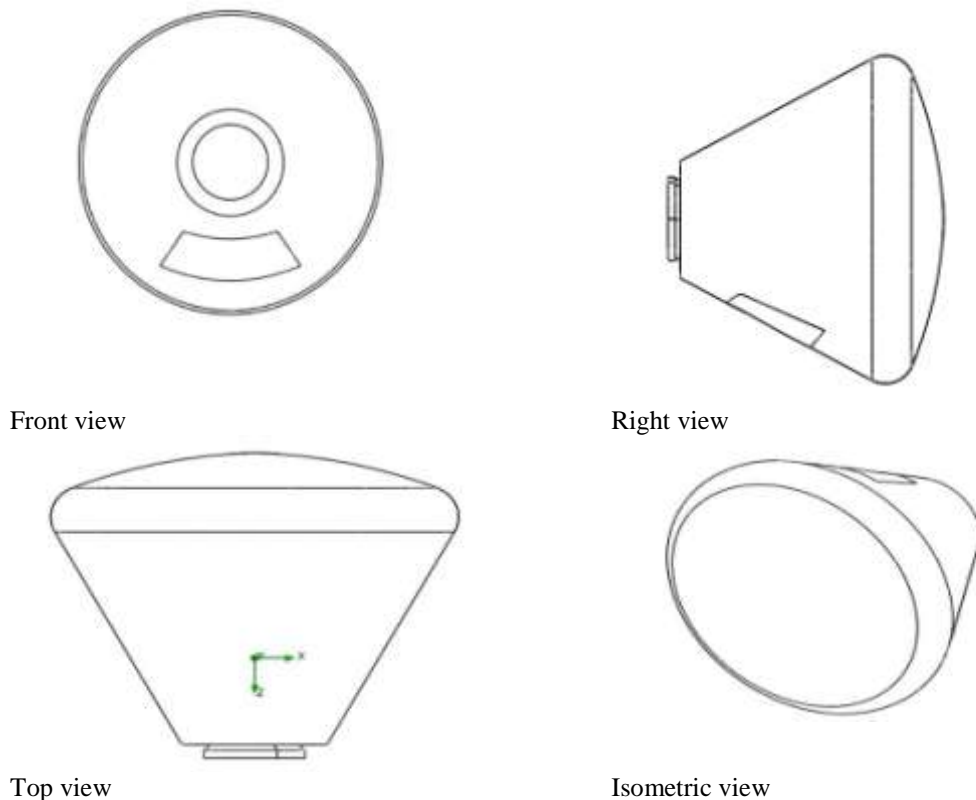


Figure 1 Design of the re-entry vehicle

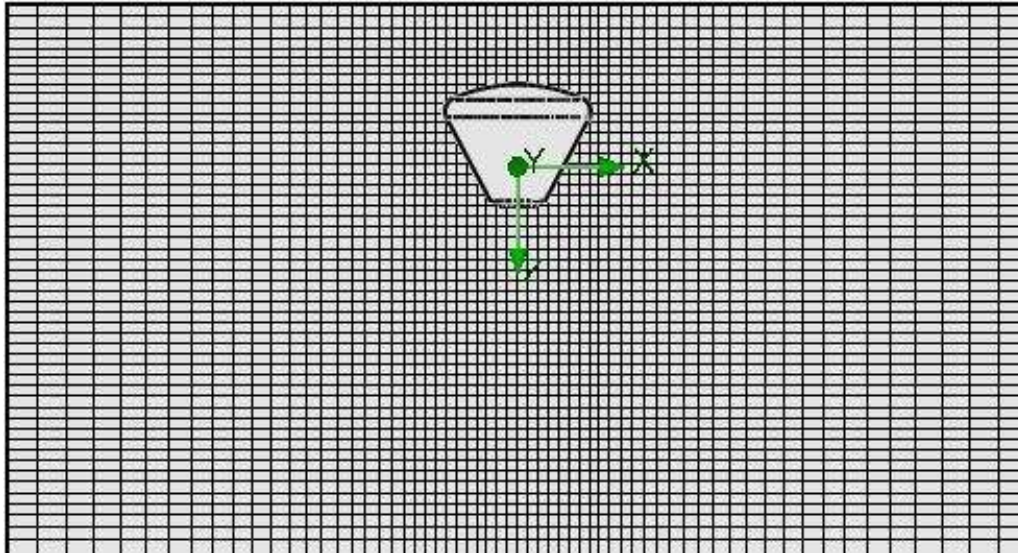


Figure 2 Grid file with re-entry vehicle and computational domain

III. MATHEMATICAL MODELLING

To solve any fluid, flow the governing equations play a key role. Mentioned below are the basic governing equations of the fluid used in the simulation process to understand the flow.

3.1 Continuity equation

$$\rho \frac{D\rho}{Dt} + \rho \Delta \cdot V = 0$$

3.2 Momentum equation

$$\rho \left(\frac{Du}{Dt} \right) = - \left(\frac{\partial p}{\partial x} \right) + \left(\frac{\partial \tau_{xx}}{\partial x} \right) + \left(\frac{\partial \tau_{yx}}{\partial y} \right) + \left(\frac{\partial \tau_{zx}}{\partial z} \right) + \rho f_x$$

3.5 Reynolds shear stress transport equations

$$\underbrace{\frac{\partial}{\partial t} (\rho \overline{u'_i u'_j})}_{\text{Local Time Derivative}} + \underbrace{\frac{\partial}{\partial x_k} (\rho u_k \overline{u'_i u'_j})}_{C_{ij} \equiv \text{Convection}} = - \underbrace{\frac{\partial}{\partial x_k} \left[\rho \overline{u'_i u'_j u'_k} + p (\delta_{kj} u'_i + \delta_{ik} u'_j) \right]}_{D_{T,ij} \equiv \text{Turbulent Diffusion}}$$

$$+ \underbrace{\frac{\partial}{\partial x_k} \left[\mu \frac{\partial}{\partial x_k} (\overline{u'_i u'_j}) \right]}_{D_{L,ij} \equiv \text{Molecular Diffusion}} - \underbrace{\rho \left(\overline{u'_i u'_k} \frac{\partial u_j}{\partial x_k} + \overline{u'_j u'_k} \frac{\partial u_i}{\partial x_k} \right)}_{P_{ij} \equiv \text{Stress Production}} - \underbrace{\rho \beta (g_i \overline{u'_j \theta} + g_j \overline{u'_i \theta})}_{G_{ij} \equiv \text{Buoyancy Production}}$$

$$+ \underbrace{p \left(\frac{\partial u'_i}{\partial x_j} + \frac{\partial u'_j}{\partial x_i} \right)}_{\phi_{ij} \equiv \text{Pressure Strain}} - \underbrace{2\mu \frac{\partial u'_i}{\partial x_k} \frac{\partial u'_j}{\partial x_k}}_{\epsilon_{ij} \equiv \text{Dissipation}}$$

$$\underbrace{-2\rho\Omega_k (\overline{u'_j u'_m} \epsilon_{ikm} + \overline{u'_i u'_m} \epsilon_{jkm})}_{F_{ij} \equiv \text{Production by System Rotation}} + \underbrace{S_{user}}_{\text{User-Defined Source Term}}$$

IV. BOUNDARY CONDITIONS

Considering the re-entry vehicle domain as wall and surrounding boundary as ideal gas air, the flow simulation is performed using shear stress

3.3 Energy equation

$$\rho \left(\frac{De}{Dt} \right) = \rho q^{\text{dot}} + \frac{\partial}{\partial x} (k \frac{\partial T}{\partial x}) + \frac{\partial}{\partial y} (k \frac{\partial T}{\partial y}) + \frac{\partial}{\partial z} (k \frac{\partial T}{\partial z}) - p \left(\frac{\partial u}{\partial x} + \frac{\partial v}{\partial y} + \frac{\partial w}{\partial z} \right) + \tau_{xx} \left(\frac{\partial u}{\partial x} \right) + \tau_{yx} \left(\frac{\partial u}{\partial y} \right) + \tau_{zx} \left(\frac{\partial u}{\partial z} \right) + \tau_{xy} \left(\frac{\partial v}{\partial x} \right) + \tau_{yy} \left(\frac{\partial v}{\partial y} \right) + \tau_{zy} \left(\frac{\partial v}{\partial z} \right) + \tau_{xz} \left(\frac{\partial w}{\partial x} \right) + \tau_{yz} \left(\frac{\partial w}{\partial y} \right) + \tau_{zz} \left(\frac{\partial w}{\partial z} \right)$$

3.4 Navier Stokes equation

$$\frac{\partial}{\partial t} (\rho \cdot u) + \frac{\partial}{\partial x} (\rho u^2) + \frac{\partial}{\partial y} (\rho uv) + \frac{\partial}{\partial z} (\rho uw) = - \frac{\partial p}{\partial x} + \frac{\partial}{\partial x} [\lambda \Delta \cdot V + 2\mu \left(\frac{\partial u}{\partial x} \right)] + \frac{\partial}{\partial y} [\mu \{ (\frac{\partial v}{\partial x}) + (\frac{\partial u}{\partial y}) \}] + \frac{\partial}{\partial z} [\mu \{ (\frac{\partial u}{\partial z}) + (\frac{\partial w}{\partial x}) \}] + \rho f_x$$

transport model at the flow velocity of 2500 m/s velocity. Table 1 shows the details of the boundary conditions taken while simulating the flow. Table 1

below describes the boundary conditions used in the problem.

S.no	Location	Value
1	Re-entry vehicle	Wall
2	Domain enclosure	Far field air ideal gas
3	Inlet velocity	2500 m/s
4	Outlet	Opening 1 atm
5	Turbulence	SST model

Table 1 Boundary conditions

V. RESULTS AND DISCUSSIONS
 By using CFD code and appropriate turbulence models, simulation has been performed to predict

the flow phenomena. Figure 3 shows the streamline around the re-entry vehicle.

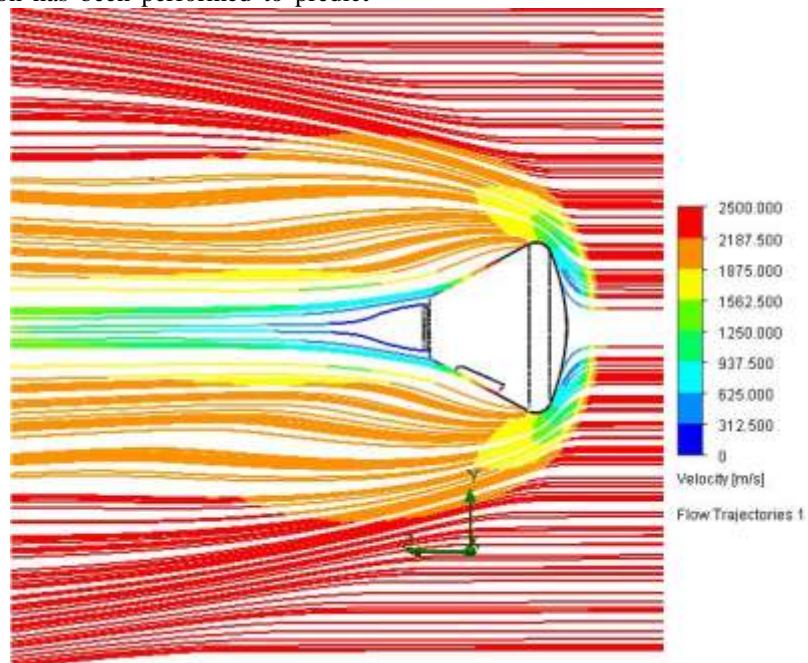


Figure 3 Streamlines around re-entry vehicles

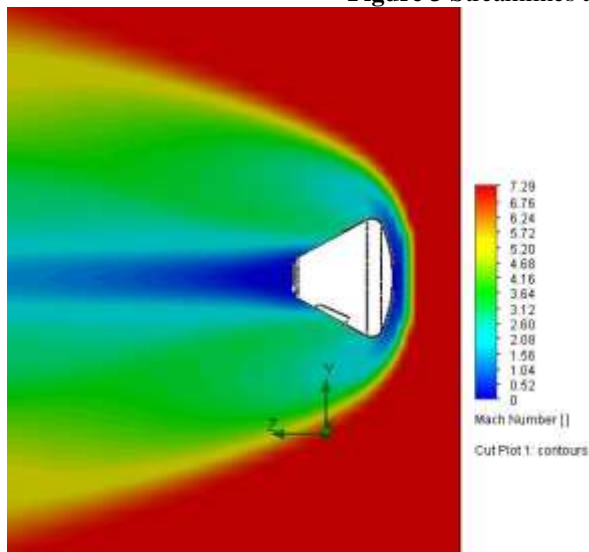


Figure 4 Contours of Mach Number

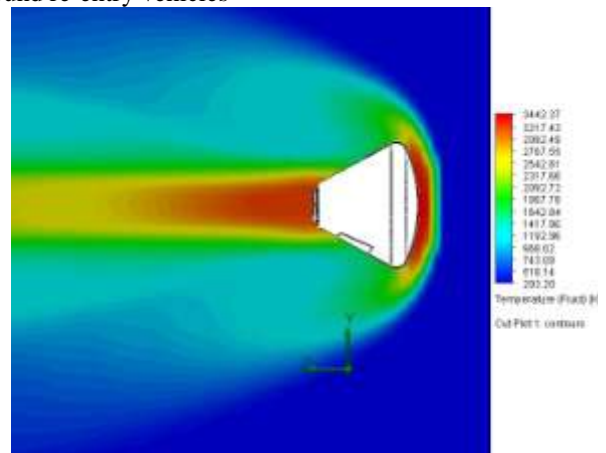


Figure 5 Contours of Static Temperature

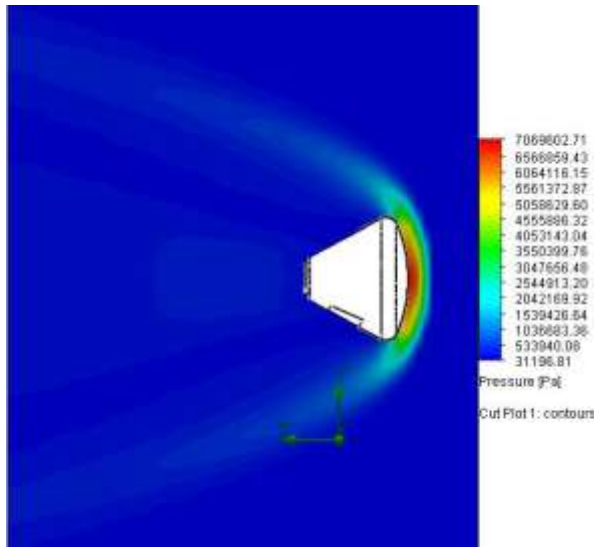


Figure 6 Contours of Static pressure

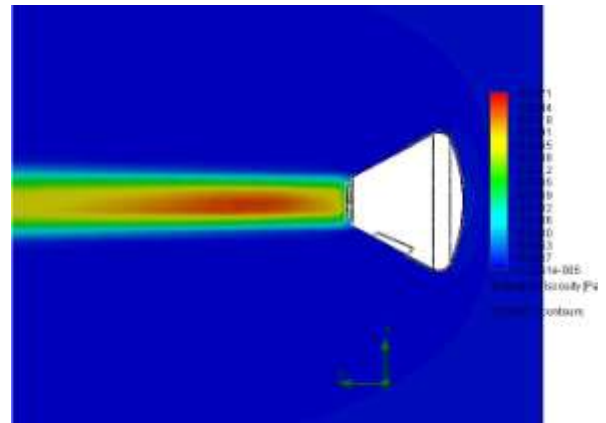


Figure 7 Contours of Turbulent viscosity

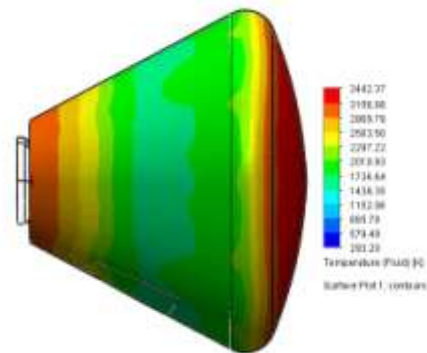
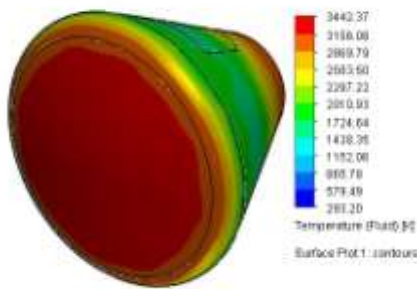


Figure 8 Contours of temperature on the re-entry vehicle

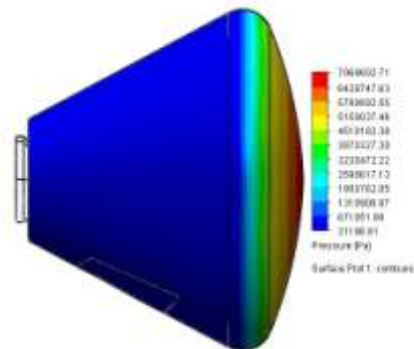
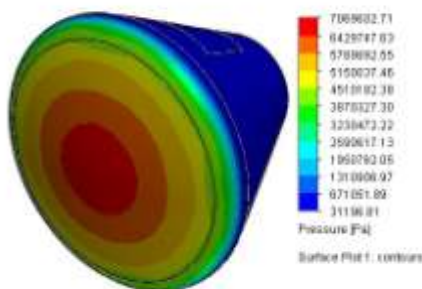


Figure 9 Contours of pressure

Property	Minimum	Maximum
Pressure [Pa]	31196.81	7069602.71
Temperature [K]	293.20	3442.37
Density [kg/m ³]	0.05	7.15
Velocity (X) [m/s]	-1104.913	1103.962
Velocity (Y) [m/s]	-1104.727	1094.048
Velocity (Z) [m/s]	-126.243	2500.000
Mach Number []	0	7.29

Shear Stress [Pa]	0	11900.76
Dynamic Viscosity [Pa*s]	1.8146e-005	9.5500e-005
Fluid Thermal Conductivity [W/(m*K)]	0.0258	0.4860
Turbulent Viscosity [Pa*s]	1.2251e-005	0.0371
Turbulent Energy [J/kg]	8.548	854472.441
Turbulent Dissipation [W/kg]	10854.92	8.80e+011

Table 2 Minimum and maximum values of the flow properties

By including all the basic flow governing equations, the flow scheme had been estimated. In figure 4 Mach number around the re-entry vehicle was plotted. A minimum value of Mach 0 was found at the end of the re-entry vehicle. Figure 6 and 9 shows the pressure variation around the re-entry vehicle with maximum pressure of 7069602 Pa at the front part of the re-entry vehicle. In table

2 all the minimum and maximum values of the flow properties have been mentioned. In figure 10 and 11 plots of temperature vs specific heat and thermal conductivity had been represented respectively.

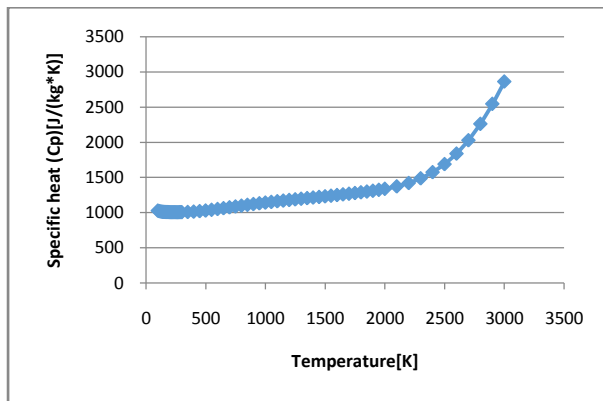


Figure 10 Specific heat vs Temperature

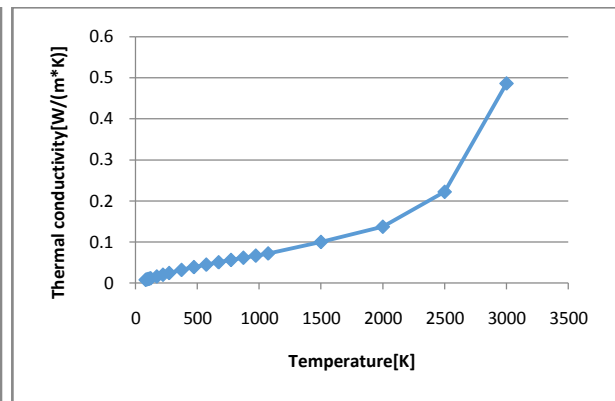


Figure 11 Thermal conductivity vs Temp

VI. CONCLUSION

Flow around the re-entry vehicle had been estimated at 2500 m/s velocity by using computer aided mathematical coding. Minimum and maximum values of the flow properties in the case were tabulated. Maximum possible pressure and temperature of 7069602 Pa and 3442 K were reported, which could be used for further structural analysis. Flow pattern was estimated by using different contours.

REFERENCES

[1]. Yusuke Takahashi, Manabu Matsunaga, Nobuyuki Oshima and Kazuhiko Yamada, "Drag Behavior of Inflatable Re-entry Vehicle in Transonic Regime", Journal of space craft and rockets, November 2018, <https://doi.org/10.2514/1.A34069>.
 [2]. Keiichiro Fujimoto, Hideyo Negishi and Ryoh Nakamuya, "Aero-Acoustics CFD Prediction for Re-entry Capsule Wake Flows at Subsonic to Supersonic Regime",

American Institute of Aeronautics and Astronautics (AIAA) Aerospace sciences meeting, January 2018, Florida, <https://doi.org/10.2514/6.2018-0520>.

[3]. Zhen-Xun Gao, Hai-Chao Xue, Zhi-Chao Zhanga, Hong-Peng Liu, Chun-Hian Lee, "A hybrid numerical scheme for aeroheating computation of hypersonic reentry vehicles", International Journal of Heat and Mass Transfer, Volume 116, January 2018, Pages 432-444, <https://doi.org/10.1016/j.ijheatmasstransfer.2017.07.100>.
 [4]. Toshiyuki Suzuki, Michiko Furudate and Keisuke Sawada, "Unified Calculation of Hypersonic Flowfield for a Reentry Vehicle", Journal of thermos physics and heat transfer, Jan – March 2002, <https://doi.org/10.2514/2.6656>.
 [5]. Yuan Xian et all, "The pitching static/dynamic derivatives computation based on CFD methods", Acta Aerodynamica Sinica, 2004-2005.

-
- [6]. J.M.A Longo, M. Orłowska, S. Brück, "Considerations on CFD modeling for the design of re-entry vehicles", *Aerospace Science and Technology*. Volume 4, Issue 5, July 2000, Pages 337-345.
 - [7]. Yan Chao et al., "Scheme effect and grid dependency in CFD computations of heat transfer", *Acta Aerodynamica Sinica*, 2005-2006.
 - [8]. Alexandre Martin and Iain Boyd, "CFD Implementation of a novel carbon-phenolic-in-air chemistry model for atmospheric re-entry", 49th AIAA Aerospace sciences meeting January 2011, <https://doi.org/10.2514/6.2011-143>.
 - [9]. Antonio Viviani and Giuseppe Pezzella, "Computational FlowField Analysis over a Blunt-Body Reentry Vehicle", *Journal of Aircraft and Rockets*.
 - [10]. Yusuke Takahashi, "Advanced validation of CFD-FDTD combined method using highly applicable solver for reentry blackout prediction", *Journal of Physics D: Applied Physics*.
 - [11]. Tian Wan et al, "CFD Modeling and Simulations of MHD Power Generation During Re-Entry", 35th AIAA Plasma dynamics and laser conference.